Macromolecules

ARTICLE

pubs.acs.org/Macromolecules

Synthesis and Properties of a Variety of Well-Defined Hyperbranched *N*-Alkyl and *N*-H Polyamides by Chain-Growth Condensation Polymerization of AB_2 Monomers

Yoshihiro Ohta, Yusuke Kamijyo, Shuichi Fujii, Akihiro Yokoyama, and Tsutomu Yokozawa*

Department of Material and Life Chemistry, Kanagawa University, Rokkakubashi, Kanagawa-ku, Yokohama 221-8686, Japan

Supporting Information

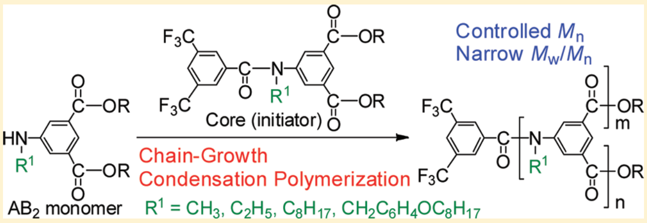

ABSTRACT: Well-defined hyperbranched polyamides (HBPAs) were synthesized by means of chain-growth condensation polymerization of AB_2 monomers from core molecules, making use of the change of substituent effects between the monomer and the polymer. Polymerization of 5-(methylamino)isophthalic acid ethyl ester **1c** as an AB_2 monomer with core **3b** was carried out in the presence of lithium 1,1,1,3,3,3-hexamethyldisilazide (LiHMDS) and LiCl in THF at −30 °C to yield HBPA with low polydispersity ($M_w/M_n \leq 1.13$) and well-defined molecular weight (M_n = 2370−39300) depending on the feed ratio of the monomer to the core (from 7 to 200). The matrix-assisted laser desorption ionization time-of-flight (MALDI−TOF) mass spectra showed that the obtained HBPA included the core unit, indicating that the polymerization proceeds by selective reaction of the monomer with the core and the polymer ends, without side reactions. Polymerization of other AB_2 monomers with *N*-ethyl, octyl, and 4-octyloxybenzyl (OOB) groups afforded the corresponding well-defined HBPAs. HBPA with the *N*-OOB group was converted to unsubstituted *N*-H HBPA with low polydispersity by treatment with trifluoroacetic acid (TFA). The solubility of HBPAs depended upon the nature of the *N*-alkyl groups and the terminal ester moieties. The glass transition temperature (T_g) and 10% weight-loss temperature (T_d^{10}) of HBPAs depended upon the molecular weight, as well as the nature of the *N*-alkyl groups and terminal ester moieties.

INTRODUCTION

Hyperbranched polymers have received considerable attention in recent years due to their unusual properties arising from their unique molecular architecture.[1−3] In contrast to the multistep syntheses of dendrimers, hyperbranched polymers can be prepared by one-step polymerization of AB_m ($m \geq 2$) type monomers, but their physical properties depend on polymer topology, molecular weight, and molecular weight distribution, which are not well controlled. Therefore, a number of studies on controlled synthesis of hyperbranched polymers have been conducted to obtain products with improved properties. For example, hyperbranched polymers with a degree of branching (DB) of 100% were synthesized by "criss-cross" cycloaddition,[4] superacid-catalyzed condensation of keto and aryl groups,[5,6] and catalyst-transfer Suzuki−Miyaura coupling polymerization of fluorene derivatives.[7] Furthermore, polymer architecture could be tuned from linear to hyperbranched by means of ethylene coordination polymerization,[8] cobalt-mediated free radical polymerization,[9] and Michael-addition polymerization.[10] Recently, the DB has been arbitrarily controlled from 0 to 100% by adjusting the amount of superacid used in the condensation reaction.[11]

Several approaches have been investigated to achieve control of the molecular weight and molecular weight distribution of hyperbranched polymers. Suzuki and co-workers carried out ring-opening isomerization polymerization of cyclic latent AB_2 monomers from a core molecule in a chain-growth polymerization manner. The M_w/M_n of the obtained polymer was 1.3−1.5 with M_n in the range from 2000 to 3000,[12,13] but when attempts were made to synthesize polymer with higher molecular weight by decreasing the amount of the initiator, the polymer precipitated. Another approach is the slow monomer addition (SMA) method,[14−17] using core molecules on an insoluble solid support[18] or highly reactive core molecules.[19] This method provided polymers with controlled molecular weight and low polydispersity ($M_w/M_n < 1.3$) when the monomer/core ratio was less than about 100. Above that ratio, however, the molecular weight distribution became broad or the deviation of the observed molecular weight from the calculated value increased even when polymers with low polydispersity were obtained. These results probably arose from self-polymerization of AB_2 monomers at high feed ratio.

Herein, we report a new approach to obtain hyperbranched polymers with controlled molecular weight and low polydispersity by living polymerization of AB_2 monomers: chain-growth condensation polymerization.[20] We focused on the change of

Received: April 29, 2011
Revised: May 20, 2011
Published: June 13, 2011

© 2011 American Chemical Society

Scheme 1

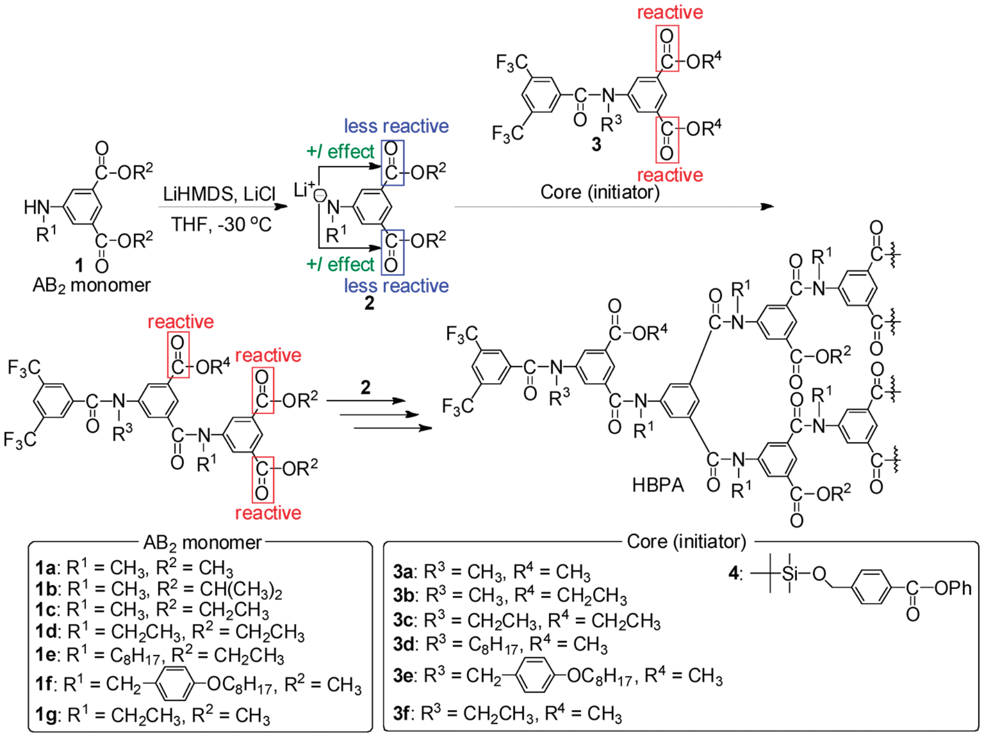

substituent effects between monomer and polymer. In the condensation polymerization of 5-(alkylamino)isophthalic acid ester (**1**) as an AB$_2$ monomer with a base, both ester moieties in the amide anion of **2** would be deactivated owing to the inductive effect (+*I* effect), thereby suppressing self-polymerization, and **2** would selectively react with the core molecule (initiator) **3** and the terminal ester moieties of the polymer to afford a well-defined hyperbranched polymer (Scheme 1), in a similar manner to that in which AB-type monomers undergo chain-growth condensation polymerization.[21] This polymerization method allowed us to synthesize a variety of hyperbranched polyamides (HBPA) with different solubility and thermal properties, such as glass tradition temperature (T_g) and 10% weight-loss temperature (T_d[10]), simply by changing the *N*-alkyl group of AB$_2$ monomers **1**. The effects of the *N*-alkyl group and the terminal ester alkyl group on the solubility, T_g, and T_d[10] of HBPAs were investigated. Furthermore, we synthesized unsubstituted *N*-H HBPA by the polymerization of **1f** bearing a N-protecting group, followed by removal of the protecting group with acid.

■ EXPERIMENTAL SECTION

Measurements. ^{1}H, ^{13}C and ^{19}F NMR spectra were obtained on JEOL ECA-600 and ECA-500 instruments operating in the pulsed Fourier-transfer (FT) mode, using tetramethylsilane (TMS, 0.00 ppm) and the midpoint of CDCl$_3$ (77.0 ppm) as internal standards of ^{1}H and ^{13}C NMR spectra, and C$_6$F$_6$ (0.00 ppm) as an external standard of ^{19}F NMR. IR spectra were recorded on a JASCO FT/IR-410. GC was performed on a Shimadzu GC-14B gas chromatograph equipped with a Shimadzu fused silica capillary column CBP1-W12−100 (12 m length, 0.53 mm i.d.) and a flame ionization detector (FID). The M_n and M_w/M_n values of polymers were measured on a Shodex GPC-101 (eluent, THF; calibration, polystyrene standards) equipped with Shodex UV-41, Shodex RI-71S, and Wyatt Technology DAWN EOS multiangle laser light scattering (MALLS, Ga−As laser, λ = 690 nm) detectors and two Shodex KF-804-L columns, and a Tosoh HLC-8220 SEC (eluent: solution of LiBr and phosphoric acid (20 mM) in DMF; calibration, polystyrene standards) equipped with refractive index and ultraviolet detectors and Shodex Asahipak GF-710 and two GF-310 columns. MALDI−TOF mass spectra were recorded on a Shimadzu/Kratos AXIMA-CFR plus in the reflectron ion mode by use of a laser (λ = 337 nm). Dithranol (1,8-dihydroxy-9[10H]-anthracenone) was used as the matrix for the MALDI−TOF mass measurements. ESI-MS experiments were performed using the high-resolution JEOL AccuTOF-CS instrument. The glass transition temperatures (T_gs) of the polymers were measured on a Seiko Instruments differential scanning calorimeter (DSC) model EXSTAR6000/DSC6200 at a heating rate of 10 °C/min under nitrogen. Thermal analysis was performed on a Seiko Instruments thermogravimetric analyzer (TGA) model EXSTAR6000/TG/DTA6200 at a heating rate of 10 °C/min under nitrogen.

Materials. A solution of lithium 1,1,1,3,3,3-hexamethyldisilazide (LiHMDS, Aldrich; 1.0 M solution in THF), dehydrated *N,N*-dimethylformamide (dry DMF, Kanto), dehydrated tetrahydrofuran (dry THF, Kanto) and dehydrated dichloromethane (dry CH$_2$Cl$_2$, Kanto) were used as received without purification. Syntheses of various AB$_2$ monomers **1**, core initiators **3**, **4**, and model compounds of dendritic and linear units are described in the Supporting Information.

Polymerization of *N*-Methyl AB$_2$ Monomer 1c with Bifunctional Initiator 3b. LiCl (0.152 g, 3.59 mmol) was placed in a flask equipped with a three-way stopcock, and dried at 250 °C under reduced pressure. The flask was cooled to room temperature under an argon atmosphere, and then charged with 1.0 M LiHMDS in THF (0.720 mL, 0.720 mmol). The flask was cooled to −30 °C under an argon atmosphere with stirring. Into the flask was added a solution of **3b** (0.0053 g, 0.0108 mmol) and naphthalene (internal standard, 0.0096 g, 0.075 mmol) in dry THF (1.0 mL) under dry nitrogen, followed by a solution of **1c** (0.163 g, 0.649 mmol) in dry THF (4.0 mL), added dropwise over ca.

40 min at −30 °C with stirring under dry nitrogen. The mixture was stirred at −30 °C for 1 h, and then the reaction was quenched with sat. NH_4Cl. A small portion of the THF layer was withdrawn into a syringe and analyzed by GC to determine the conversion of **3b** and **1c** (conversion = 100%). After that, the whole was extracted with CH_2Cl_2. The organic layer was washed with water, dried over anhydrous $MgSO_4$, and concentrated under reduced pressure. The residue was dissolved in CH_2Cl_2 (2.0 mL), and the solution was added to hexane (150 mL). After filtration, the insoluble material was washed with hexane, and dried in desiccator to give poly**1c** as a white solid (0.113 g, 82%, M_n(MALLS) = 13500, M_w/M_n = 1.11).

Polymerization of *N*-Ethyl AB$_2$ Monomer 1d with Bifunctional Initiator 3c. LiCl (0.154 g, 3.64 mmol) was placed in a flask equipped with a three-way stopcock, and dried at 250 °C under reduced pressure. The flask was cooled to room temperature under an argon atmosphere, and then charged with 1.0 M LiHMDS in THF (0.720 mL, 0.720 mmol). The flask was cooled to −30 °C under an argon atmosphere with stirring. Into the flask was added a solution of **3c** (0.0106 g, 0.0210 mmol) and naphthalene (internal standard, 0.0128 g, 0.0999 mmol) in dry THF (1.0 mL) under dry nitrogen, followed by a solution of **1d** (0.173 g, 0.652 mmol) in dry THF (4.0 mL), added dropwise over ca. 40 min at −30 °C with stirring under dry nitrogen. The mixture was stirred at −30 °C for 1 h, and then the reaction was quenched with sat. NH_4Cl. A small portion of the THF layer was withdrawn into a syringe and analyzed by GC to determine the conversion of **3c** and **1d** (conversion = 100%). After that, the whole was extracted with CH_2Cl_2. The organic layer was washed with water, dried over anhydrous $MgSO_4$, and concentrated under reduced pressure. The residue was dissolved in CH_2Cl_2 (4.0 mL), and the solution was added to hexane/ether = 9/1 (v/v) (200 mL). After filtration, the insoluble material was washed with hexane, and dried in desiccator to give 0.132 g of poly**1d** as a white solid (86%, M_n(MALLS) = 6780, M_w/M_n = 1.13).

Polymerization of *N*-Octyl AB$_2$ Monomer 1e with Bifunctional Initiator 3d. LiCl (0.152 g, 3.59 mmol) was placed in a flask equipped with a three-way stopcock, and dried at 250 °C under reduced pressure. The flask was cooled to room temperature under an argon atmosphere, and then charged with 1.0 M LiHMDS in THF (0.720 mL, 0.720 mmol). The flask was cooled to −30 °C under an argon atmosphere with stirring. Into the flask was added a solution of **3d** (0.0116 g, 0.0207 mmol) and naphthalene (internal standard, 0.0105 g, 0.0819 mmol) in dry THF (1.0 mL) under dry nitrogen, followed by a solution of **1e** (0.218 g, 0.652 mmol) in dry THF (4.0 mL), added dropwise over ca. 45 min at −30 °C with stirring under dry nitrogen. The mixture was stirred at −30 °C for 1 h, and then the reaction was quenched with sat. NH_4Cl. A small portion of the THF layer was withdrawn into a syringe and analyzed by GC to determine the conversion of **3d** and **1e** (conversion =100%). After that, the whole was extracted with CH_2Cl_2. The organic layer was washed with water, dried over anhydrous $MgSO_4$, and concentrated under reduced pressure. The residue was purified by flash chromatography on silica gel (hexane/ethyl acetate =3/1, ethyl acetate) to give 0.165 g of poly**1e** as a yellow solid (78%, M_n(MALLS) = 9090, M_w/M_n = 1.16).

Polymerization of *N*-4-Octyloxybenzyl (OOB) AB$_2$ Monomer 1f with Bifunctional Initiator 3e. LiCl (0.154 g, 3.63 mmol) was placed in a flask equipped with a three-way stopcock, and dried at 250 °C under reduced pressure. The flask was cooled to room temperature under an argon atmosphere, and then charged with 1.0 M LiHMDS in THF (0.720 mL, 0.720 mmol). The flask was cooled to −30 °C under an argon atmosphere with stirring. Into the flask was added a solution of **3e** (0.0141 g, 0.0211 mmol) and naphthalene (internal standard, 0.0098 g, 0.076 mmol) in dry THF (1.0 mL) under dry nitrogen, followed by a solution of **1f** (0.277 g, 0.648 mmol) in dry THF (4.0 mL), added dropwise over ca. 45 min at −30 °C with stirring under dry nitrogen. The mixture was stirred at −30 °C for 3 h, and then the reaction was quenched with sat. NH_4Cl. A small portion of the THF layer was withdrawn into a syringe and analyzed by GC to determine the conversion of **3e** and **1f** (conversion = 100%). After that, the whole was extracted with CH_2Cl_2. The organic layer was washed with water, dried over anhydrous $MgSO_4$, and concentrated under reduced pressure. The residue was purified by flash chromatography on silica gel (hexane/ethyl acetate = 3/1, ethyl acetate) to give 0.232 g of poly**1f** as a slightly yellow solid (86%, M_n(MALLS) = 11600, M_w/M_n = 1.13).

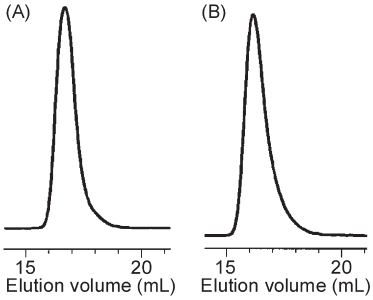

Figure 1. GPC profiles of poly**1b** obtained by the polymerization of **1b** with **3a** ($[\mathbf{1b}]_0/[\mathbf{3a}]_0$ = (A) 31 and (B) 60).

Synthesis of *N*-Unsubstituted HBPA via Deprotection of Poly1f. A solution of *N*-OOB HBPA (poly**1f**) (M_n(MALLS) = 3920, M_w/M_n = 1.08) (0.311 g, 0.0793 mmol) in trifluoroacetic acid (TFA) (5.0 mL) was stirred at room temperature for 3 days and then concentrated in vacuo, and the residue was washed CH_2Cl_2. The product was dissolved in DMF, and the solution was added to ether. The precipitate was collected through filtration and dried in a desiccator to give 0.119 g of *N*-unsubstituted HBPA as a white solid (79%).

RESULTS AND DISCUSSION

Study of the Ester Moiety of *N*-Methyl AB$_2$ Monomers. The polymerization of simple methyl ester monomer **1a** with **4** as a monofunctional core initiator was first carried out by addition of **1a** over 40 min to a mixture of 1.1 equiv of lithium 1,1,1,3,3,3-hexamethyldisilazide (LiHMDS), 3.2 mol % of **4**, and 5 equiv of LiCl in THF at −30 °C, and further stirring at −30 °C for 1 h yielded HBPA (poly**1a**) with low polydispersity (M_w/M_n = 1.20), although unreacted initiator **4** remained (conversion of **4** = 50%). However, the observed M_n value of HBPA, estimated by ^{1}H NMR (M_n(^{1}H NMR)), was close to the theoretical value (M_n(calcd)) based on the molar ratio of monomer **1a** to the converted initiator **4** (M_n(calcd) = 12100, M_n(^{1}H NMR) = 11500) (Figure S1, Supporting Information).[22] This result implied that the polymerization of **1a** from the consumed core **4** proceeded in a chain-growth polymerization manner. We then used bifunctional core initiator **3a** instead of monofunctional **4** to improve the initiation efficiency. Indeed, the conversion of **3a** was increased to 91%, and HBPA with a narrow molecular weight distribution was formed, but unreacted core initiator **3a** still remained. Even when feed ratio of **1a** to **3a** was increased, a small amount of **3a** remained (Table S1, Supporting Information).

We speculated that propagation of the polymerization of **1a** would be too fast to allow consumption of all of initiator **3a**, and that decrease of the reactivity of the ester moiety of the monomer would lead to consumption of all the initiator. To test this idea, isopropyl ester monomer **1b** was polymerized with 3.2 mol % of **3a** at −30 °C for 5 h. Indeed, **3a** was completely consumed, and HBPA (poly**1b**) with a narrow molecular weight distribution (M_w/M_n = 1.14) was obtained (Figure 1A). The M_n value of

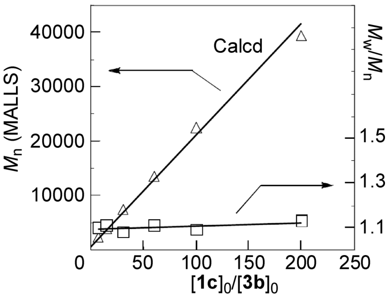

Figure 2. M_n and M_w/M_n values of poly**1c** as a function of the feed ratio of **1c** to **3b**.

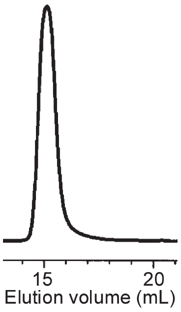

Figure 3. GPC profile of poly**1c** obtained by the polymerization of **1c** with **3b** ($[\mathbf{1c}]_0/[\mathbf{3b}]_0$ = 200).

hyperbranched polymer estimated by GPC is generally lower than the real M_n value and therefore the M_w value was determined with a multiangle laser light scattering (MALLS) detector. To facilitate comparison with the theoretical value (M_n(calcd)) based on the monomer/core feed ratio, the M_n value designated as M_n(MALLS) was calculated by division of the M_w value from MALLS by the M_w/M_n ratio from GPC. The M_n(MALLS) of the obtained HBPA was 7220, which was in good agreement with the theoretical value (M_n(calcd) = 7320). The polymerization was then carried out with increasing $[\mathbf{1b}]_0/[\mathbf{3a}]_0$ ratio from 31 to 60, but the M_n value of the obtained HBPA (M_n(MALLS) = 9010) did not reach the expected value (M_n(calcd) = 13700), and the polydispersity became slightly broader (M_w/M_n = 1.21) (Figure 1B) (Table S2, Supporting Information). This result might be accounted for by decreased reactivity of the terminal isopropyl ester moieties of higher-molecular-weight HBPA owing to steric congestion.

Accordingly, ethyl ester monomer **1c** was polymerized with 1.7 mol % of **3b** ($[\mathbf{1c}]_0/[\mathbf{3b}]_0$ = 60), yielding HBPA (poly**1c**) with a very low polydispersity (M_w/M_n = 1.11). The M_n value of the obtained HBPA (M_n(MALLS) = 13500) is in fair agreement with the calculated value, assuming that one core molecule forms one HBPA molecule (M_n(calcd) = 12800). Furthermore, when the polymerization of **1c** was carried out with various feed ratios of **1c** to **3b** ($[\mathbf{1c}]_0/[\mathbf{3b}]_0$), the observed M_n value of the poly**1c** increased in proportion to the $[\mathbf{1c}]_0/[\mathbf{3b}]_0$ ratio up to 200, retaining narrow polydispersity (Figure 2). The GPC chromatogram of poly**1c** obtained even at the monomer/core feed ratio of 200 showed a very narrow, monomodal peak (Figure 3). Consequently, it turns out that the ethyl ester monomer **1c** is the most appropriate for controlled synthesis of HBPA.

Polymer End Groups and Degree of Branching. The polymer end groups of poly**1c** were analyzed by matrix-assisted laser desorption ionization time-of-flight (MALDI–TOF) mass spectrometry with dithranol as a matrix in the presence of sodium trifluoroacetate as a cationizing salt. The mass spectrum of the poly**1c** (M_n(MALLS) = 3920, M_w/M_n = 1.11), obtained by the polymerization of **1c** with 6.7 mol % of **3b** ($[\mathbf{1c}]_0/[\mathbf{3b}]_0$ = 15), contains only one series of peaks corresponding to the Na^+ adduct of poly**1c** with the core **3b** unit (Figure 4). For example, the exact mass signal of a single isotope of the 17-mer with core **3b** unit and Na^+ is expected to appear at 4000.29 Da, and in fact a signal was observed at 3999.82 Da, as shown in the magnified spectrum in Figure 4. Furthermore, the MALDI–TOF mass spectra of the poly**1c** samples obtained during polymerization also contain only one series of peaks (Figure 5). These results

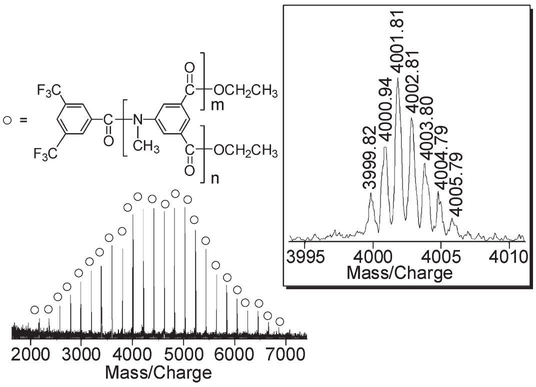

Figure 4. MALDI–TOF mass spectra of poly**1c** obtained by the polymerization of **1c** onto **3b** ($[\mathbf{1c}]_0/[\mathbf{3b}]_0$ = 15).

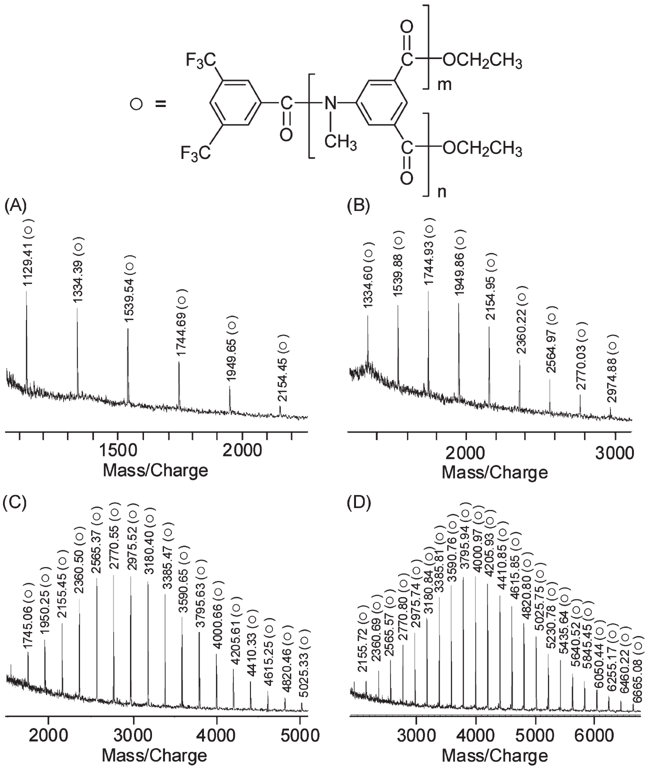

Figure 5. MALDI–TOF mass spectra of poly**1c** samples obtained during addition of **1c** into the reaction mixture of 1.1 equiv of LiHMDS and 5 equiv of LiCl in THF ($[\mathbf{1c}]_0/[\mathbf{3b}]_0$ = 15, $[\mathbf{1c}]_0$ = 0.11 M) at (A) $^1/_8$, (B) $^1/_4$, (C) $^1/_2$, and (D) $^3/_4$ of **1c** added.

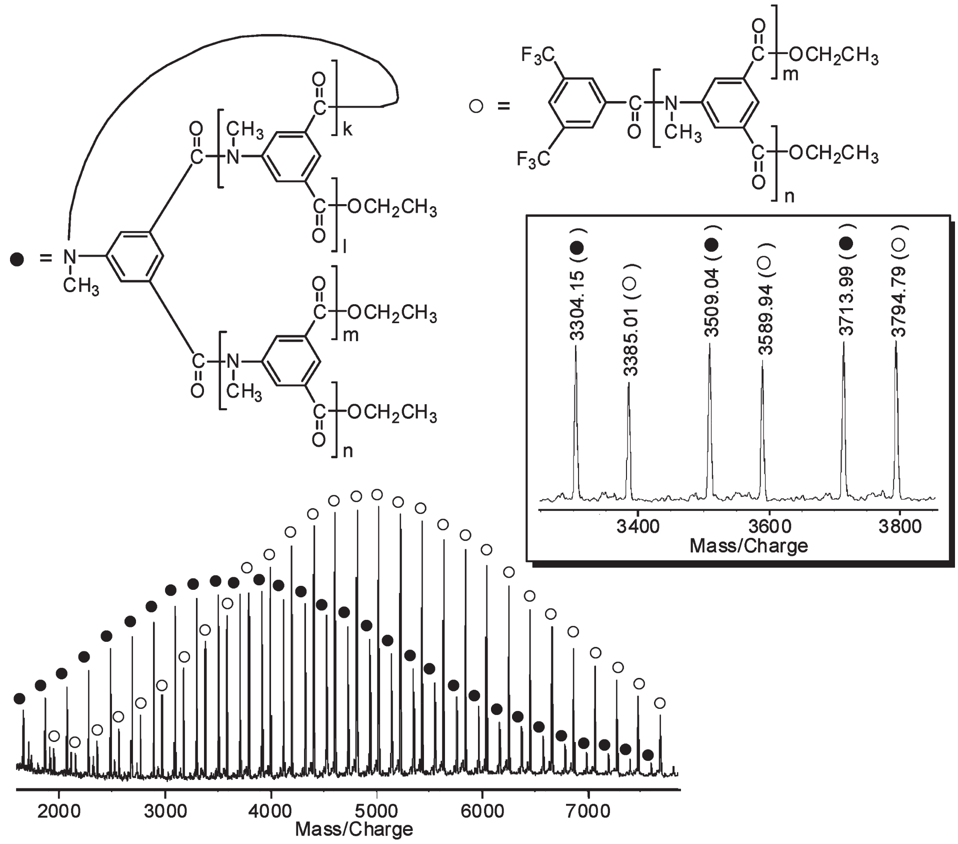

Figure 6. MALDI−TOF mass spectra of products obtained by the polymerization of **1c** with **3b** in the absence of LiCl ($[\mathbf{1c}]_0/[\mathbf{3b}]_0 = 15$).

indicate that the polymerization of **1c** proceeds in a chain-growth condensation polymerization manner from the core **3b**.

To estimate the DB of poly**1c**, model compounds of the dendritic and linear units were synthesized, and the ^{1}H NMR spectrum of poly**1c** was compared with those of the model compounds (Figure S2, Supporting Information). The ^{1}H NMR spectrum of poly**1c** showed separately the signals of the dendritic (D), linear (L), and terminal (T) units, and the DBs of poly**1c** with different M_n calculated by use of the Fréchet formula[23] were 0.49−0.52 (Table S3, Supporting Information), which are close to the theoretical value of 0.5 in the general polymerization of an AB$_2$ monomer.[24] Furthermore, the DBs of poly**1c** obtained by sampling during polymerization were also kept 0.5, implying that this HBPA has a homogenously branched structure from the core to the shell.

Effect of Monomer Addition. Since the AB$_2$ monomer **1c** was added to a mixture of the core **3b** and base for 40 min in this polymerization, one might think that the chain-growth polymerization from the core would stem from not the changed substituent effects, but from slow monomer addition (SMA), although it took more than 12 h for controlled synthesis of hyperbranched polymers by the reported SMA method.[14−17] Accordingly, the polymerization of **1c** was carried out by addition of **1c** and **3b** ($[\mathbf{1c}]_0/[\mathbf{3b}]_0 = 15$) at once to a mixture of LiHMDS and LiCl. The obtained HBPA also possessed well-controlled molecular weight and low polydispersity (M_n(MALLS) = 3450 (M_n(calcd) = 3570), M_w/M_n = 1.17) (Figure S3, Supporting Information). This result indicates that this controlled polymerization of AB$_2$ monomer is governed not by SMA, but by the change of substituent effects between the monomer and the polymer.

Effect of LiCl. In order to clarify the effect of LiCl on the polymerization, **1c** was polymerized with 6.7 mol % of **3b** ($[\mathbf{1c}]_0/[\mathbf{3b}]_0 = 15$) in the absence of LiCl. The molecular weight distribution of the obtained HBPA became broader (M_w/M_n = 1.28) (Figure S4). The MALDI−TOF mass spectrum contains two series of peaks, one corresponding to the Na$^+$ adducts of HBPA with the core **3b** unit and the other arising from HBPA without the **3b** unit, in which the amino group has intramolecularly reacted with one of the ester moieties to form a cyclic structure (Figure 6). This result means that the polymerization of **1c** without LiCl involves not only selective reaction of **1c** with **3b** and the polymer ends, but also self-polymerization of **1c**. We also checked when the self-polymerization had set in during polymerization by examining aliquots of the reaction mixture withdrawn during addition of **1c** to the mixture of LiHMDS and **3b**. The MALDI−TOF mass spectra showed only the peaks due to HBPA with the **3b** core unit until a quarter of the **1c** had been added (Figure 7, parts A and B), and clear peaks corresponding to self-polymerization appeared when a half of the **1c** had been added (Figure 7, parts C and D). It should be noted that selective reaction of **1c** with **3b** and the polymer ends took place in the initial stage, and was accompanied by self-polymerization from the middle stage. This behavior might be accounted for by slowing-down of proton abstraction from the amino group of **1c** as the base concentration decreased from the middle stage. Self-polymerization would be initiated by the reaction of **1c**, not the deprotonated compound, with the amide anion generated from **1c**, because the amide anion site strongly deactivates the ester moieties of **1c** to prevent deprotonated **1c** from reacting with itself. Therefore, slow generation of the amide anion provides

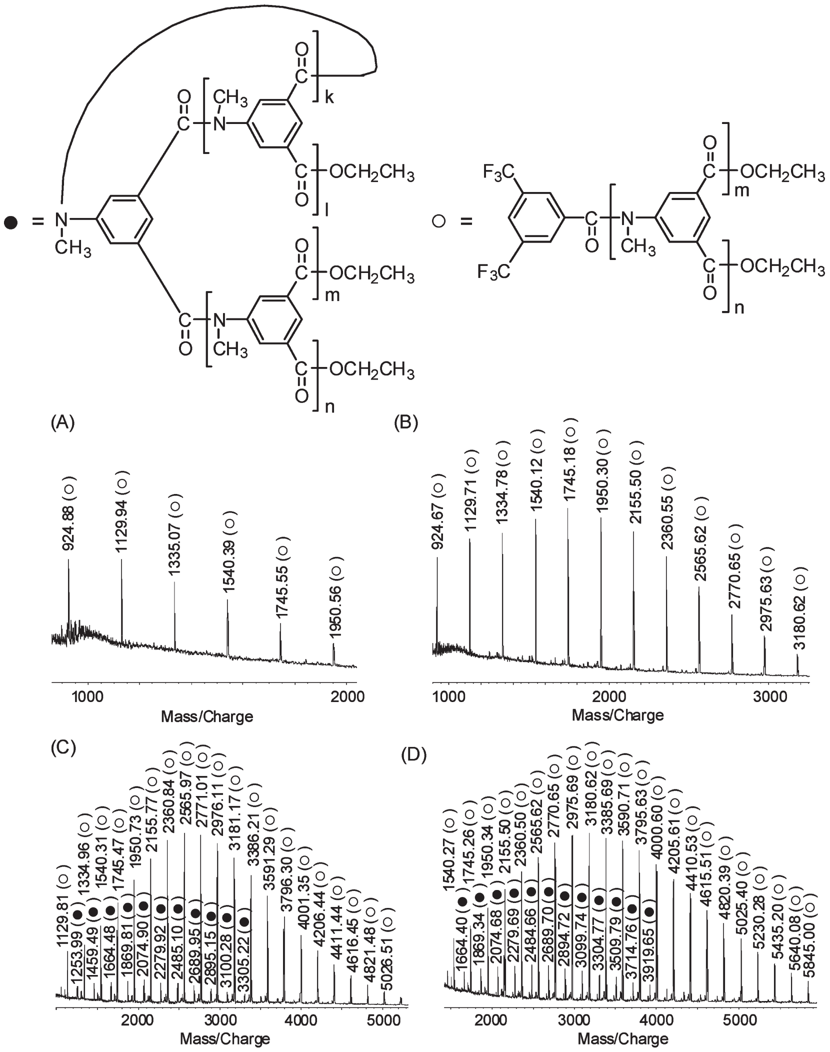

Figure 7. MALDI−TOF mass spectra of product samples obtained during addition of **1c** into the reaction mixture of 1.1 equiv of LiHMDS in THF ($[\mathbf{1c}]_0/[\mathbf{3b}]_0$ = 15) at (A) $^1/_8$, (B) $^1/_4$, (C) $^1/_2$, and (D) $^3/_4$ of **1c** added.

a greater opportunity for reaction of the amide anion with the ester moiety of **1c** (not deprotonated), which leads to self-polymerization. In the presence of LiCl, however, the reactivity of the amide anion was decreased, as shown in living anionic polymerization of methyl methacrylate in the presence of LiCl,[25] so that the reaction of the amide anion stabilized with LiCl with the ester moiety of **1c** would be prevented, resulting in selective reaction of the amide anion with **3b** and the polymer ends, i.e., chain-growth condensation polymerization.

Polymerization of Other *N*-Alkyl AB$_2$ Monomers. Since it turned out that *N*-methyl AB$_2$ monomer **1c** undergoes chain-growth condensation polymerization, we next tried to polymerize AB$_2$ monomers with a variety of *N*-alkyl groups to synthesize HBPAs with different properties. *N*-Ethyl monomer **1d** was first polymerized with 3.2 mol % of **3c** in the presence of 1.1 equiv of LiHMDS and 5 equiv of LiCl in THF at −30 °C, and further stirring at −30 °C for 1 h afforded HBPA (poly**1d**) with a well-defined M_n and a narrow molecular weight distribution (M_n(MALLS) = 6780 (M_n(calcd) = 7300), M_w/M_n = 1.13). When the polymerization of **1d** was conducted with various feed ratios of **1d** to **3c** ($[\mathbf{1d}]_0/[\mathbf{3c}]_0$), the M_n value of the HBPA increased in proportion to the $[\mathbf{1d}]_0/[\mathbf{3c}]_0$ ratio up to 50, and the polydispersity remained narrow (Figure 8A and Figure S5, Supporting Information). The DB of poly**1d**s was 0.38−0.40, which was lower than that of poly**1c**s (Table S4, Supporting Information).

A longer *N*-alkyl group, the octyl group, was introduced into AB$_2$ monomer, and the polymerization of *N*-octyl **1e** was carried out with **3d** with various feed ratios ($[\mathbf{1e}]_0/[\mathbf{3d}]_0$) in the range of 7−46, yielding HBPA (poly**1e**) with a narrow molecular weight distribution and well-controlled molecular weight, depending on the feed ratio (Figure 8B and Figure S6, Supporting Information). The DB of poly**1e**s was 0.32−0.37, which was even lower than that of poly**1d**s (Table S5, Supporting Information). These results suggest that the DB of HBPA depends on the length of the *N*-alkyl group of HPBA: a longer alkyl chain decreases the DB. Steric hindrance of the longer alkyl chain is probably the reason for this observation.

To obtain an unsubstituted *N*-H HBPA with low polydispersity, AB$_2$ monomer **1f** having the *N*-4-octyloxybenzyl (OOB) group as a protecting group was polymerized with various feed ratios of **1f** to **3e** ($[\mathbf{1f}]_0/[\mathbf{3e}]_0$). It should be noted that the methyl ester monomer **1f**, which is easier to prepare than the corresponding ethyl ester, resulted in consumption of all the

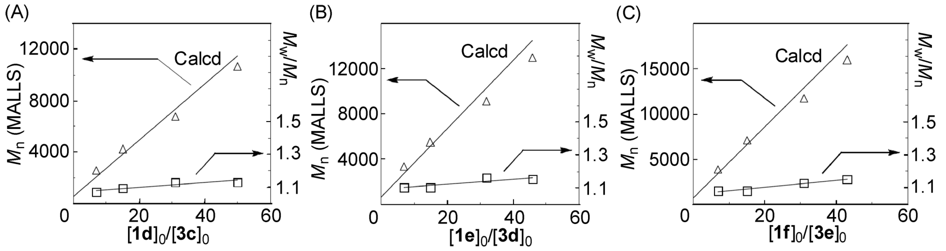

Figure 8. M_n and M_w/M_n values of HBPA as a function of the feed ratio of (A) **1d** to **3c**, (B) **1e** to **3d**, and (C) **1f** to **3e**.

Scheme 2

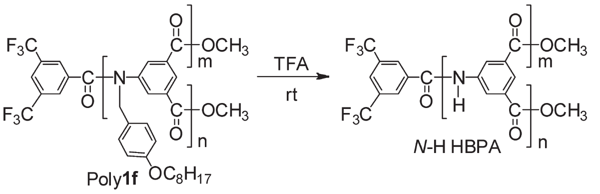

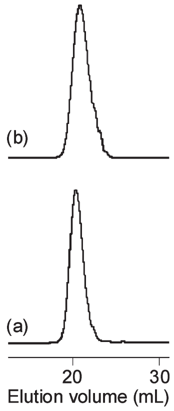

Figure 9. GPC (eluent: DMF) profiles of (a) poly**1f** (M_n = 3570, M_w/M_n = 1.05) and (b) *N*-H HBPA obtained by treatment of poly**1f** with TFA (M_n = 3000, M_w/M_n = 1.08).

initiator during polymerization. This is because the bulky OOB group on the amino group would make the propagation slow enough to allow consumption of all the initiator. The M_n value of HBPA (poly**1f**) increased in proportion to the $[\mathbf{1f}]_0/[\mathbf{3e}]_0$ ratio up to 43, and the polydispersity remained narrow (Figure 8C and Figure S7, Supporting Information; Table S6, Supporting Information). The DB of poly**1f**s was not determined, because the signals of the D, L, and T units did not separately appear in the ^{1}H NMR spectra of poly**1f**s.

The OOB group on the amide nitrogen of poly**1f** was removed with trifluoroacetic acid (TFA) at room temperature for 3 days, and then the product was purified by precipitation into ether (Scheme 2). The GPC elution curves (eluent: DMF) of the product obtained by TFA treatment were slightly shifted toward the lower molecular weight region, and low polydispersity was retained (Figure 9 and Figure S8, Supporting Information). In the ^{1}H NMR spectra of the product, the signals of the octyl protons of the OOB group of HBPA at around 3.75 and 1.75–0.9 ppm disappeared, and a new signal due to amide N–H proton was observed at around 11 ppm (Figure 10). Furthermore, signals of the Na^+ or K^+ adduct of HBPA involving a secondary amide linkage (*N*-H HBPA) were observed in MALDI–TOF mass spectra of the product (Figure 11). For example, the exact mass of a single isotope of the 8-mer of *N*-H HBPA with Na^+ and K^+ is expected to produce signals at 1888.38 and 1904.35 Da, respectively, and indeed, signals were observed at 1888.41 and 1904.36 Da. These results indicate that quantitative removal of the OOB group on the amide nitrogen of poly**1f** occurred without scission of the amide linkage, leading to *N*-H HBPA with a narrow molecular weight distribution.

Solubility of HBPA. The solubility of HBPA with the *N*-methyl group (poly**1c**) was first compared with that of the corresponding *N*-methyl linear poly(*m*-benzamide) (*N*-Me-*m*-LPA).[26] Poly**1c** was freely soluble in the reaction solvent, THF, during polymerization even at the feed ratio of **1c** to core initiator **3b** of 200, whereas *N*-Me-*m*-LPA was precipitated during polymerization at the feed ratio of ethyl 3-(methylamino)benzoate to initiator of more than 10.0. This difference in solubility is thought to reflect the difference in polymer architecture: hyperbranched polymer is generally more soluble than linear polymer.

The solubility of poly**1c** and *N*-Me-*m*-LPA in other solvents was next examined (Table 1). Poly**1c** was soluble in toluene, but *N*-Me-*m*-LPA was insoluble. In contrast, poly**1c** was insoluble in polar solvents such as methanol and ethanol, in which *N*-Me-*m*-LPA was soluble. This difference might be due to the difference in the number of terminal ester moieties. The solubility of *N*-Me-*m*-LPA, having only one terminal ethyl ester moiety, is affected by the polar amide linkage of the backbone, whereas the solubility of poly**1c** is governed by the many nonpolar terminal ester moieties. In addition, *N*-methyl HBPAs with different terminal ester moieties (poly**1a**, methyl ester; poly**1c**, ethyl ester; poly**1b**, isopropyl ester) showed different solubilities.

The effect of the *N*-alkyl group of HBPA was also studied. *N*-Methyl HBPA (poly**1c**) and *N*-ethyl HBPA (poly**1d**) are insoluble in ether, in which *N*-octyl HBPA (poly**1e**) is soluble. This solubility tendency is similar to that of the corresponding *N*-alkyl poly(*m*-benzamide)s.[26] Furthermore, when four HBPAs with *N*-methyl or ethyl and terminal methyl or ethyl ester, poly**1a** (*N*-methyl, methyl ester), poly**1c** (*N*-methyl, ethyl ester), poly**1d** (*N*-ethyl, ethyl ester), poly**1g** (*N*-ethyl, methyl ester),[27] were compared, the solubility was found to decrease in the order of poly**1d**, poly**1c**, poly**1g**, and poly**1a**. This result suggests that the solubility of HBPA is more affected by the alkyl group of the ester moiety than by the *N*-alkyl group, if both alkyl groups are the same. The observed propensity can be attributed to a stronger effect of the outer ester alkyl group of HBPA on the solubility, compared to the inner *N*-alkyl group of the amide linkage.

N-H HBPA was found to be soluble in DMF at room temperature and DMSO on heating. Since linear *N*-H poly(*m*-benzamide) (*N*-H-*m*-LPA) is soluble in DMF and DMSO at room temperature,[26] *N*-H HBPA is somewhat less soluble than

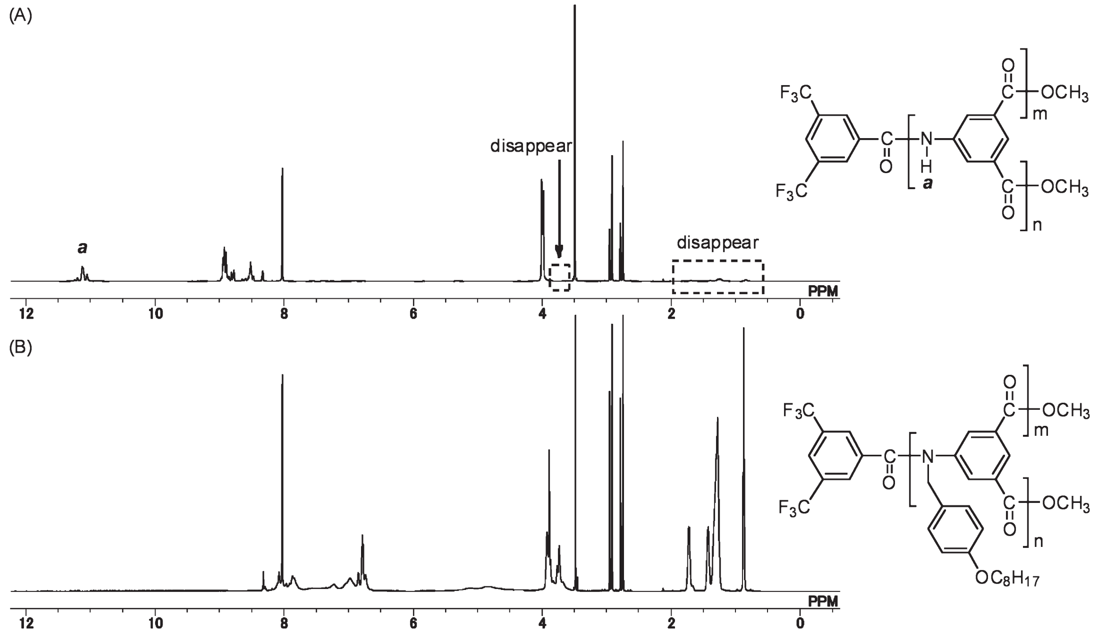

Figure 10. ^{1}H NMR spectra of (A) *N*-H HBPA obtained by treatment of poly**1f** with TFA and (B) poly**1f** in DMF-d_7 at 25 °C.

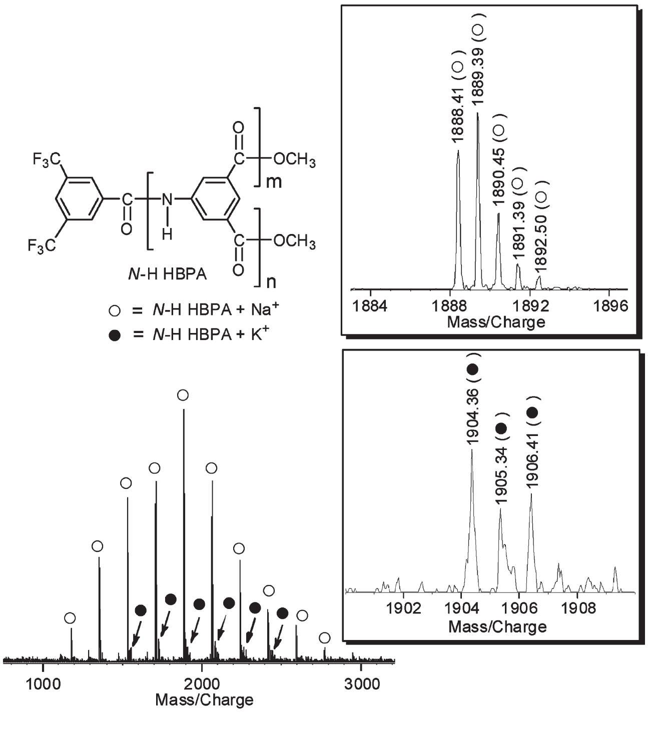

Figure 11. MALDI–TOF mass spectra of *N*-H HBPA obtained by treatment of poly**1f** with TFA at room temperature.

N-H-*m*-LPA; this is the opposite tendency to that in the solubility of linear and hyperbranched polymers. We speculate that *N*-H-*m*-LPA may be dissolved in a certain conformation, but *N*-H HBPA has reduced flexibility to adopt such a conformation.

Thermal Properties of HBPA. Since all HBPAs in hand possess well-controlled molecular weight and low polydispersity, we can evaluate precisely the molecular weight dependency of the glass transition temperature (T_g) and the 10% weight-loss temperature (T_d^{10}) of HBPA. We first investigated the effect of the molecular weight of HBPA on T_g (Figure 12). The T_g values of HBPAs in Figure 12 increased with increasing molecular weight up to 10000, and the T_g values of *N*-methyl HBPAs (poly**1a** and poly**1c**) leveled off when the M_n value was higher than about 20000. This tendency of the T_g to approach a limiting value is similar to the reported behavior of hyperbranched polyesters[28] and polyethers,[29] and dendritic polyethers and polyesters.[30] Wooley and Fréchet et al. accounted for this T_g behavior of dendritic macromolecules in terms of a modified chain-end free volume theory using eq 1 where n_e is the number of chain ends, $T_{g\infty}$ is the value of T_g extrapolated to infinite molecular weight, and K is a constant.[30] We examined whether our observed molecular weight dependency of the T_g of HBPAs could be accounted for by this modified chain-end free volume theory. First, the n_e/M_n value was plotted as a function of degree of polymerization (DP) of poly**1c** (Figure 13). The n_e/M_n value turned out to be constant when the DP was more than 100. This tendency is consistent with the limiting value of T_g at M_n more than 20000 (the DP is about 100). The T_g of poly**1c** was then plotted as a function of $[(n_e/M_n) - (n_e/M_n)_\infty]$ using the $(n_e/M_n)_\infty$ value obtained in Figure 13 (Figure 14). This gave a good linear plot, and $T_{g\infty} = 125.6$ was obtained as the y-intercept ($[(n_e/M_n) - (n_e/M_n)_\infty] = 0$). This value is in good agreement with the experimental value (122 °C) of the T_g of HBPA with M_n more than 20000. Therefore, it turns out that the molecular weight dependency of the T_g of HBPA can be well described by the modified chain-end free volume theory.

$$T_g = T_{g\infty} - K\left[(n_e/M) - (n_e/M)_\infty\right] \qquad (1)$$

We next examined the effect of the *N*-alkyl group and the terminal ester alkyl group on the T_g of HBPA. When we compared the T_g values of *N*-methyl HBPA and *N*-ethyl HBPA with similar M_n and the same terminal ester alkyl groups (methyl ester HBPAs, poly**1a** vs poly**1g**; ethyl ester HBPAs, poly**1c** vs poly**1d**), the T_g value of *N*-methyl HBPAs was about 15 °C

Table 1. Solubility of HBPAs and *N*-Methyl Poly(*m*-benzamide)[a]

solvent	*N*-Me-*m*-LPA	poly**1a**(Me/Me)[b]	poly**1c** (Me/Et)[b]	poly**1b** (Me/*i*-Pr)[b]	poly**1d** (Et/Et)[b]	poly**1g** (Et/Me)[b]	poly**1e** (Oct/Et)[b]
hexane	−	−	−	−	−	−	−
ether	−	−	−	−	−	−	++
toluene	−	−	++	++	++	+	++
CH_2Cl_2	++	++	++	++	++	++	++
ethyl acetate	+	++	++	++	++	++	++
acetone	++	++	++	++	++	++	++
CH_3CN	++	++	++	++	++	++	++
DMF	++	++	++	++	++	++	++
DMSO	++	++	++	++	++	++	+
ethanol	+	−	−	++	+	−	+
methanol	++	−	−	++	+	−	−

[a] Key: ++, soluble at room temperature; +, soluble on heating; −, insoluble. [b] *N*-Alkyl group/ester alkyl group.

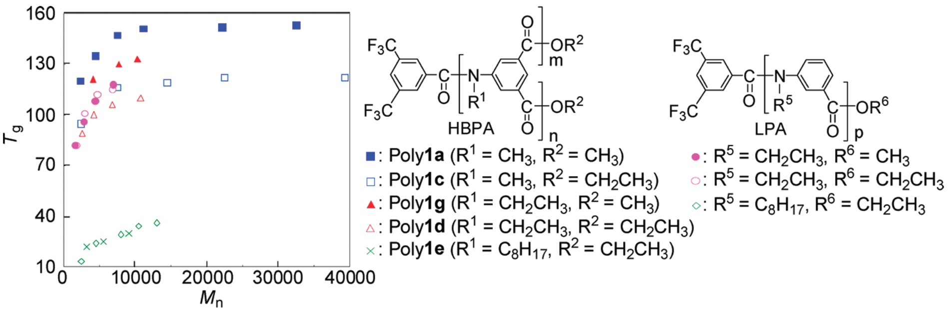

Figure 12. T_g of HBPA and LPA as a function of M_n of HBPA and LPA.

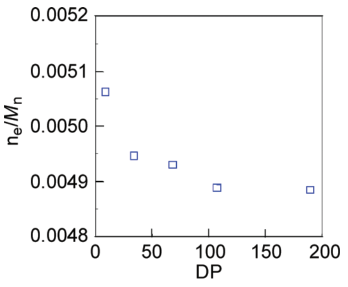

Figure 13. n_e/M_n as a function of degree of polymerization of poly**1c**.

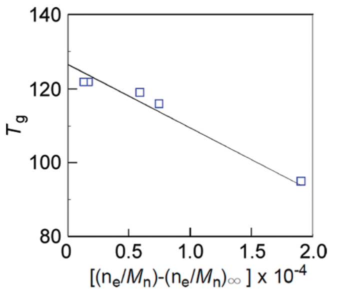

Figure 14. T_g of poly**1c** as a function of $[(n_e/M_n) - (n_e/M_n)_\infty]$.

higher than that of *N*-ethyl HBPAs. The T_g value of *N*-octyl HBPA was as low as 30 °C or less, being about 80 °C lower than that of *N*-ethyl HBPA (poly**1e** vs poly**1d**). On the other hand, when we compared the T_g values of the methyl ester and ethyl ester HBPAs with similar M_n and the same *N*-alkyl groups (*N*-methyl HBPAs, poly**1a** vs poly**1c**; *N*-ethyl HBPAs, poly**1g** vs poly**1d**), the T_g value of the methyl ester HBPAs is about 25 °C higher than that of the ethyl ester HBPAs. These results suggest that the T_g of HBPA is more influenced by the terminal ester alkyl group than by the *N*-alkyl group. This is similar to the aforementioned observation of the effect of the terminal ester alkyl group and the *N*-alkyl group on the solubility of HBPA; the terminal ester alkyl group presumably has more mobility than the *N*-alkyl group of the amide linkage, resulting in a greater effect of the terminal ester alkyl group on the T_g of HBPA. For *N*-H HBPA with terminal methyl ester moieties, the T_g is more than 200 °C.

We also compared the T_g of *N*-ethyl and octyl HBPAs with those of the corresponding linear *N*-alkyl poly(*m*-benzamide)s (LPAs). As mentioned above, the T_g value of *N*-ethyl HBPA with methyl ester terminal groups is about 25 °C higher than that of the ethyl ester counterpart, whereas the T_g values of *N*-ethyl poly(*m*-benzamide)s are almost the same, irrespective of the methyl ester and ethyl ester terminal groups (filled red circles vs red circles in Figure 12). This difference is predictable, and is due to the difference in the numbers of terminal groups between hyperbranched polymers and linear polymers. The T_g values of *N*-ethyl poly(*m*-benzamide)s are intermediate between the T_g values of *N*-ethyl HBPA with the methyl ester terminal groups and the ethyl ester counterpart. Meanwhile, the T_g values of *N*-octyl HBPA and *N*-octyl poly(*m*-benzamide) are identical, implying that the T_g values of aromatic polyamides with long *N*-alkyl groups would not be affected by the polymer topology.

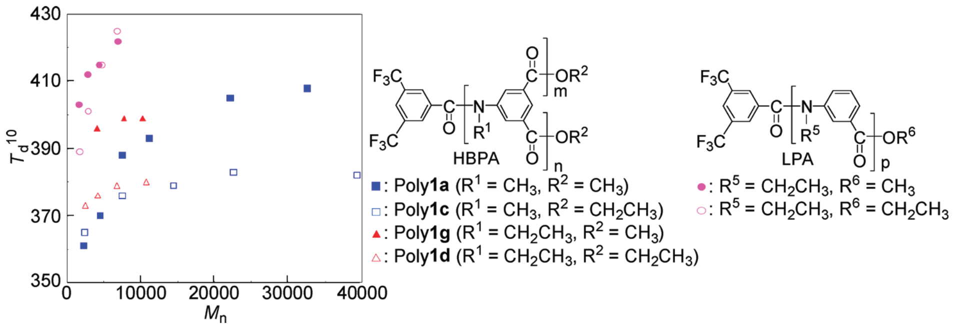

Figure 15. T_d^{10} of HBPA and LPA as a function of M_n of HBPA and LPA.

The T_d^{10} of *N*-methyl and ethyl HBPAs with methyl and ethyl ester moieties was investigated (Figure 15). All the T_d^{10} values increased with increasing molecular weight of HBPAs. The T_d^{10} value of the methyl ester HBPA is higher than that of the ethyl ester HBPA with the same *N*-alkyl group (*N*-methyl, poly**1a** vs poly**1c**; *N*-ethyl, poly**1g** vs poly**1d**), which is similar to the case of T_g, whereas the T_d^{10} value of *N*-methyl HBPA is lower than that of *N*-ethyl HBPA with the same terminal ester alkyl group, which is the opposite tendency to that in the case of T_g (methyl ester HBPAs, poly**1a** vs poly**1g**; ethyl ester HBPAs, poly**1c** vs poly**1d**). The reason for this observation is not clear at present. When we compared *N*-ethyl HBPA (poly**1g** and poly**1d**) with *N*-ethyl poly(*m*-benzamide)s of similar molecular weight, the T_d^{10} values of the HBPAs are much lower than those of the poly(*m*-benzamide)s, and this can be ascribed to different numbers of ester moieties that are thermally degradable.

CONCLUSION

We have demonstrated that well-defined HBPAs with *N*-methyl, ethyl, octyl, and 4-octyloxybenzyl (OOB) moieties can be synthesized by means of chain-growth condensation polymerization of AB_2 monomer **1** using core initiator **3**. To ensure consumption of all of the core initiator **3** in the polymerization of **1**, the choice of the ester moieties in **1** was found to be critical. In the case of *N*-methyl HBPA, polymerization of the methyl ester monomer **1a** was occurred too quickly for all of the initiator **3a** to be consumed, whereas the ethyl ester monomer **1c** was polymerized with consumption of all the core initiator, yielding HBPA with low polydispersity and well-controlled molecular weight corresponding to the monomer-to-core feed ratio up to 200. Furthermore, MALDI−TOF mass spectrometry indicated that LiCl in the reaction mixture served to suppress self-polymerization of **1c**. Well-defined *N*-H HBPA was synthesized by removal of the OOB group from *N*-OOB HBPA with TFA.

The solubility of HBPAs is influenced by the *N*-alkyl group and the terminal ester alkyl group; the effect of the latter alkyl group on the solubility is greater than that of the former alkyl group. The T_g value of HBPAs increased with increasing molecular weight and leveled off at the DB of about 100. The T_g is also influenced by the *N*-alkyl group and the terminal ester alkyl group. In other words, HBPA with defined T_g can be synthesized by tuning the *N*-alkyl group and the terminal ester alkyl group. The T_d^{10} of HBPAs is about 360−400 °C, depending on the molecular weight, *N*-alkyl group, and terminal ester alkyl group, but is lower than that of the corresponding *N*-alkyl poly(*m*-benzamide)s. This lower T_d^{10} of HBPAs can be ascribed to thermal decomposition of the many terminal ester moieties of HBPAs. Further studies on synthesis and properties of novel architectures containing well-defined HBPA on the basis of chain-growth condensation polymerization of AB_2 monomers in a living polymerization manner are in progress.

ASSOCIATED CONTENT

Supporting Information. Text and schemes giving synthetic procedures for the AB_2 monomer, bifunctional core initiator and model compounds, figures showing ^{1}H NMR spectra of model compounds and HBPA and GPC profiles of the HBPA, and tables summarizing the results of polymerization of **1**. This material is available free of charge via the Internet at http://pubs.acs.org/.

AUTHOR INFORMATION

Corresponding Author

*E-mail: yokozt01@kanagawa-u.ac.jp. Telephone: +81-45-481-5661. Fax: +81-45-413-9770.

ACKNOWLEDGMENT

This work was supported in part by a Grant-in-Aid (19550128) for Scientific Research and a Scientific Frontier Research Project grant from the Ministry of Education, Culture, Sports, Science and Technology, Japan.

REFERENCES

(1) Kim, Y. H. *J. Polym. Sci., Part A: Polym. Chem.* **1998**, *36*, 1685.
(2) Voit, B. I.; Lederer, A. *Chem. Rev.* **2009**, *109*, 5924.
(3) Gao, C.; Yan, D. *Prog. Polym. Sci.* **2004**, *29*, 183.
(4) Maier, G.; Zech, C.; Voit, B.; Komber, H. *Macromol. Chem. Phy.* **1998**, *199*, 2655.
(5) Smet, M.; Schacht, E.; Dehaen, W. *Angew. Chem., Int. Ed.* **2002**, *41*, 4547.
(6) Sinananwanich, W.; Ueda, M. *J. Polym. Sci., Part A: Polym. Chem.* **2008**, *46*, 2689.
(7) Huang, W.; Su, L.; Bo, Z. *J. Am. Chem. Soc.* **2009**, *131*, 10348.
(8) Guan, Z.; Cotts, P. M.; McCord, E. F.; McLain, S. J. *Science* **1999**, *283*, 2059.
(9) Guan, Z. *J. Am. Chem. Soc.* **2002**, *124*, 5616.
(10) Hong, C.-Y.; You, Y.-Z.; Wu, D.-C.; Liu, Y.; Pan, C.-Y. *J. Am. Chem. Soc.* **2007**, *129*, 5354.
(11) Segawa, Y.; Higashihara, T.; Ueda, M. *J. Am. Chem. Soc.* **2010**, *132*, 11000.
(12) Suzuki, M.; Ii, A.; Saegusa, T. *Macromolecules* **1992**, *25*, 7071.
(13) Suzuki, M.; Yoshida, S.; Shiraga, K.; Saegusa, T. *Macromolecules* **1998**, *31*, 1716.

(14) Sunder, A.; Hanselmann, R.; Frey, H.; Mülhaupt, R. *Macromolecules* **1999**, *32*, 4240.

(15) Bharathi, P.; Moore, J. S. *Macromolecules* **2000**, *33*, 3212.

(16) Möck, A.; Burgath, A.; Hanselmann, R.; Frey, H. *Macromolecules* **2001**, *34*, 7692.

(17) Kainthan, R. K.; Muliawan, E. B.; Hatzikiriakos, S. G.; Brooks, D. E. *Macromolecules* **2006**, *39*, 7708.

(18) Bharathi, P.; Moore, J. S. *J. Am. Chem. Soc.* **1997**, *119*, 3391.

(19) Bernal, D. P.; Bedrossian, L.; Collins, K.; Fossum, E. *Macromolecules* **2003**, *36*, 333.

(20) For a preliminary report, see: Ohta, Y.; Fujii, S.; Yokoyama, A.; Furuyama, T.; Uchiyama, M.; Yokozawa, T. *Angew. Chem., Int. Ed.* **2009**, *48*, 5942.

(21) Yokozawa, T.; Yokoyama, A. *Chem. Rev.* **2009**, *109*, 5595.

(22) M_n(^{1}H NMR) was determined on the basis of the average value of degree of polymerization of HBPA, which calculated from the integral ratio of N-CH_3 signal **b** in the repeat unit of HBPA to the signal **a** of the benzyl methylene signal from **4** (Figure S1, Supporting Information).

(23) Hawker, C. J.; Lee, R.; Fréchet, J. M. J. *J. Am. Chem. Soc.* **1991**, *113*, 4583.

(24) Frey, H.; Hölter, D. *Acta Polym.* **1999**, *50*, 67.

(25) Varshney, S. K.; Hautekeer, J. P.; Fayt, R.; Jerome, R.; Teyssie, P. *Macromolecules* **1990**, *23*, 2618.

(26) Ohishi, T.; Sugi, R.; Yokoyama, A.; Yokozawa, T. *J. Polym. Sci., Part A: Polym. Chem.* **2006**, *44*, 4990.

(27) Synthesis of poly**1g**, see Supporting Information; the results are summarized there in Figure S9 and Table S7.

(28) Parker, D.; Feast, W. J. *Macromolecules* **2001**, *34*, 2048.

(29) Behera, G. C.; Ramakrishnan, S. *Macromolecules* **2004**, *37*, 9814.

(30) Wooley, K. L.; Hawker, C. J.; Pochan, J. M.; Fréchet, J. M. J. *Macromolecules* **1993**, *26*, 1514.